ORIGINAL RESEARCH

Chronic Hypoxia in an EXTrauterine Environment for Neonatal Development Impairs Lung Development

Maureen Peers de Nieuwburgh[1,2,3], Mallory Hunt[5], Prashant Chandrasekaran[3], Tiffany L. Vincent[4], Kevin B. Hayes[1], Isabel R. Randazzo[1], Meredith Gunder[1], Felix R. De Bie[1], Arthur Colson[6,7], Minqi Lu[3], Hongbo Wen[3], Sylvia N. Michki[3,4], Jack Rychik[3], Fréderic Debième[6,7], Jeremy Katzen[8], Lisa R. Young[4], Marcus G. Davey[9], Alan W. Flake[1], J. William Gaynor[2]*, and David B. Frank[3]*

[1]Center for Fetal Research, [2]Division of Cardiac Surgery, Department of Surgery, [3]Division of Cardiology, [4]Division of Pulmonology and Sleep Medicine, Department of Pediatrics, Children's Hospital of Philadelphia, University of Pennsylvania, Philadelphia, Pennsylvania; [5]Division of Cardiovascular Surgery, Department of Surgery, Hospital of the University of Pennsylvania, Philadelphia, Pennsylvania; [6]Pôle de Recherche en Physiopathologie de la Reproduction, Institut de Recherche Expérimentale et Clinique, and [7]Service d'Obstétrique, Cliniques Universitaires Saint-Luc, Université Catholique de Louvain, Brussels, Belgium; [8]Division of Pulmonary and Critical Care Medicine, Department of Medicine, University of Pennsylvania, Philadelphia, Pennsylvania; and [9]Vitara Biomedical, Inc., Philadelphia, Pennsylvania

ORCID IDs: 0000-0003-0403-0648 (S.N.M.); 0000-0002-3064-2069 (D.B.F.).

Abstract

Severe fetal hypoxia poses a significant risk to lung development, resulting in severe postnatal complications. Existing chronic hypoxia animal models lack the ability to achieve pathologically reduced fetal oxygen without compromising animal development, placental blood flow, or maternal health. Using an established model of isolated chronic hypoxia involving the Extrauterine Environment for Neonatal Development, we are able to investigate the direct impact of fetal hypoxia on lung development. Oxygen delivery to preterm fetal lambs (105–110 d gestational age) delivered by cesarean section was reduced, and animals were supported using the Extrauterine Environment for Neonatal Development through the canalicular or saccular stage of lung development. Fetal lambs in hypoxic conditions showed significant growth restriction compared with their normoxic counterparts. We also observed modest aberrant vascular remodeling in the saccular group after hypoxic conditions, with decreased macrovessel numbers and microvascular endothelial cell numbers and increased peripheral vessel muscularization. In addition, fetal hypoxia resulted in enlarged distal airspaces and decreased septal wall volume. Moreover, there was a reduction in mature SFTPB (surfactant protein B) and processed SFTPC protein expression concomitant with a decrease in alveolar type 2 cell number. These findings demonstrate that maternally independent fetal hypoxia predominantly affects distal airway development, alveolar type 2 cell number, and surfactant production, with mild effects on the vasculature.

Keywords: hypoxia; extracorporeal membrane oxygenation; fetal sheep; EXTEND; lung development

(Received in original form January 11, 2024; accepted in final form October 23, 2024)

*Co-senior authors.

Supported by the Children's Hospital of Philadelphia Academic Development Fund and the Daniel M. Tabas, Alice Langdon Warner, and Mortimer J. Buckley, Jr., M.D., Endowed Chairs in Pediatric Cardiothoracic Surgery and by grants K08HL140129 and R56HL167937 (D.B.F.), K08HL150226 (J.K.), and R01HL119503 and K24HL143281 (L.R.Y.). M.P.d.N. benefits from the financial support from the French Community of Belgium through a scholarship from the Fund for Research training in Industry and Agriculture.

Author Contributions: M.P.d.N., M.H., M.G., J.W.G., A.W.F., M.G.D., and D.B.F. conceived the project. M.P.d.N., D.B.F., J.W.G., A.W.F., F.D., and M.G.D. designed the experiments. M.P.d.N., P.C., K.B.H., I.R.R., J.R., A.C., F.R.D.B., M.L., S.N.M., T.L.V., J.K., F.D., H.W., and D.B.F. conducted experiments and/or contributed to data analysis and interpretation. M.P.d.N., P.C., J.R., F.D., L.R.Y., M.G.D., A.W.F., J.W.G., and D.B.F. contributed to the writing and editing of the manuscript.

Correspondence and requests for reprints should be addressed to David B. Frank, M.D., Ph.D., Division of Cardiology, Department of Pediatrics, Perelman School of Medicine at the University of Pennsylvania, 3615 Civic Center Boulevard, ARC 416K, Philadelphia, PA 19104. E-mail: frankd@chop.edu.

This article has a data supplement, which is accessible at the Supplements tab.

Am J Respir Cell Mol Biol Vol 72, Iss 4, pp 441–452, April 2025

Originally Published in Press as DOI: 10.1165/rcmb.2024-0012OC on October 25, 2024
Internet address: www.atsjournals.org

Clinical Relevance

This study answers the long-standing question as to whether chronic hypoxia directly affects lung development or is a consequence of intrauterine growth restriction, maternal compromise, or placental flow. Using the EXTrauterine Environment for Neonatal Development has the potential to improve outcomes of prematurity. Moreover, the system provides a model for testing the direct effects of oxygen toxicity or deficits on organ development.

Oxygen tension in the fetus plays a critical role in lung development. During a healthy pregnancy, fetal arterial blood oxygen saturation increases progressively to reach 60% during the second trimester (1). This low oxygen saturation, compared with children or adults, is an essential mediator of lung endodermal and mesodermal development and an important regulator of vascular development (2, 3). However, conditions causing decreased fetal oxygen tension, called severe fetal hypoxia, can also lead to important lung complications responsible for acute respiratory distress, such as perinatal asphyxia, bronchopulmonary dysplasia, and persistent pulmonary hypertension of the newborn (PPHN) (4, 5).

A significant obstacle in studying the consequences of severe fetal hypoxia in animal models is the inability to attain pathologically reduced fetal oxygen delivery without compromising nutritional delivery, affecting cardiac afterload, or inducing maternal stress, which can result in additional intrauterine growth restriction (IUGR) complications (6). Current research is also complicated by variation in the timing, severity, and duration of exposure to hypoxia as well as the animal model used (7, 8). Thus, there is an unfulfilled need to improve models of isolated fetal hypoxia to understand its effect on lung development during gestation.

Recently, an artificial womb called the Extrauterine Environment for Neonatal Development (EXTEND) was developed to provide up to four weeks of physiologic support for extreme preterm lambs (9, 10). This system is designed to mimic the physiologic conditions of the womb as if the preterm lamb were still in its mother's uterus (9). EXTEND consists of a closed fluid environment called a "biobag" in which the preterm lamb is immersed in synthetic amniotic fluid and oxygenated via its umbilical cord with a pumpless arteriovenous circuit. In these initial studies, all organs at risk of sustaining complications due to premature birth developed normally during the incubation period and well into adult life (9, 11). Although this has broad implications for the management of prematurity, it also allows the study of toxic oxygen tension levels on the developing fetus independent of the potential contribution of maternal effects. Given the vast amount of data supporting aberrant postnatal lung development and injury in the presence of hypoxia, we hypothesized that isolated fetal hypoxia contributes directly to the disruption of lung development. Using the EXTEND system, these studies will be the first to clarify the role of direct hypoxia in aberrant remodeling and injury during lung development.

Methods

Additional details on methods and protocols used to maintain lambs on EXTEND and to measure all analyses listed below can be found in the data supplement.

Animal Model

All procedures were approved by the Institutional Animal Care and Use Committee of the Children's Hospital of Philadelphia (IAC 19-01212). The methods for surgical procedures for EXTEND have been previously described (9, 12). Once on EXTEND, lambs were randomly divided into hypoxic and normoxic groups independently of sex. The hypoxic group experienced gradual reduction in oxygen delivery (~14 ml/kg/min) after 24 hours on EXTEND to mimic severe fetal hypoxia (13). The normoxic group received physiologic fetal oxygen delivery (~20 ml/kg/min) and served as the control group. The length of stay on EXTEND was either 7 days (canalicular stage of lung development) or 14–21 days (saccular stage of lung development). In the canalicular stage group, hypoxic and normoxic groups consisted of five lambs each. In the saccular stage group, six animals were included in the hypoxic group and four to five animals in the normoxic group. All 21 lambs involved in this study successfully completed the designated end-of-study protocols. Lambs that were excluded from the study either experienced premature death or underwent highly complicated runs on EXTEND, clearly standing out as outliers within the group. Once end of protocol was met, animals were weighed, and the heart and lungs were isolated and removed for further analyses.

Histopathological Analysis

Lung morphometrical analysis (14), including mean linear intercept, absolute volume of alveolar septa, and vascular medial wall thickness, was performed after hematoxylin and eosin and Verhoeff's elastin staining, respectively. Immunohistochemistry (IHC) with specific antibodies was used to measure peripheral vascular muscularization, macrovascular number, microvascular endothelial cell (EC) count, and alveolar type 2 (AT2) cell quantification.

mRNA Quantification in the Fetal Lung

Expression of genes regulating hypoxia signaling and surfactant maturation was measured using quantitative PCR (qPCR). Previously published primers are summarized in Table E1 in the data supplement (15–17). Results are expressed as fold change after calculation using the $\Delta\Delta$CT method relative to the canalicular normoxic group.

Protein Quantification and Western Blot in the Fetal Lung

Protein identification and quantification were done using western blotting primary antibodies used for both western blotting and IHC can be found in Table E2, followed by secondary antibody incubation, developed using 20X LumiGLO Reagent and 20X peroxide (catalog #7003; Cell Signaling Technology).

Fetal Lung Tissue Cortisol Concentration

Fetal lung cortisol was extracted and quantified according to a previously published protocol (18).

Statistical Analysis

Hemodynamic and oxygen parameters were averaged over 24-hour intervals. Hypoxic animals' size markers, vital signs, ultrasound parameters, and lung analysis were compared

with those of normoxic animals using between-group analysis with the two-tailed unpaired *t* test or Mann-Whitney test. Normal distribution was assessed using the Shapiro-Wilk test ($P < 0.05$) for all analysis. Significance was accepted at $P < 0.05$, and data are presented as mean ± SEM. Data points were considered outliers if the point differed by more than 2 SDs from other data points in the same study group.

Results

EXTEND-mediated Hypoxia Affects Physiological and Growth Parameters

To create an isolated chronic hypoxic environment, we used the previously published EXTEND model that allows extrauterine survival and the ability to titrate oxygen (Figure 1A) (9, 19–23). Day 106–111 gestational age lambs were exposed to hypoxia and harvested at later time points consistent with the canalicular stage ($n = 5$) and saccular stage ($n = 6$) of lamb lung development. Control animals were placed under normoxic conditions and harvested at the same canalicular ($n = 5$) and saccular ($n = 5$) stages (*see* Table E3). There were no major technical complications during cannulation, and all lambs were successfully transitioned to EXTEND. All animals were killed at the end of protocol. While on EXTEND, lambs underwent continuous hemodynamic and oxygen parameter monitoring (*see* Table E3). To obtain severe fetal hypoxia, we controlled oxygenation parameters to decrease oxygen delivery by 25–30% in the hypoxic group compared with normoxic counterparts. We confirmed fetal hypoxia with decreased oxygen delivery and decreased partial pressure of oxygen in the hypoxic group as well increased lactic acid (Figures 1B, 1C, and E1A). Umbilical arterial pH was kept stable in both study groups via the administration of buffered fluid infusion or the intermittent administration of sodium bicarbonate to the hypoxic cohort (see Table E3).

To assess physiologic and functional outcomes of isolated fetal hypoxia, we performed measures of hemodynamics and growth. We performed daily echocardiographic examinations that

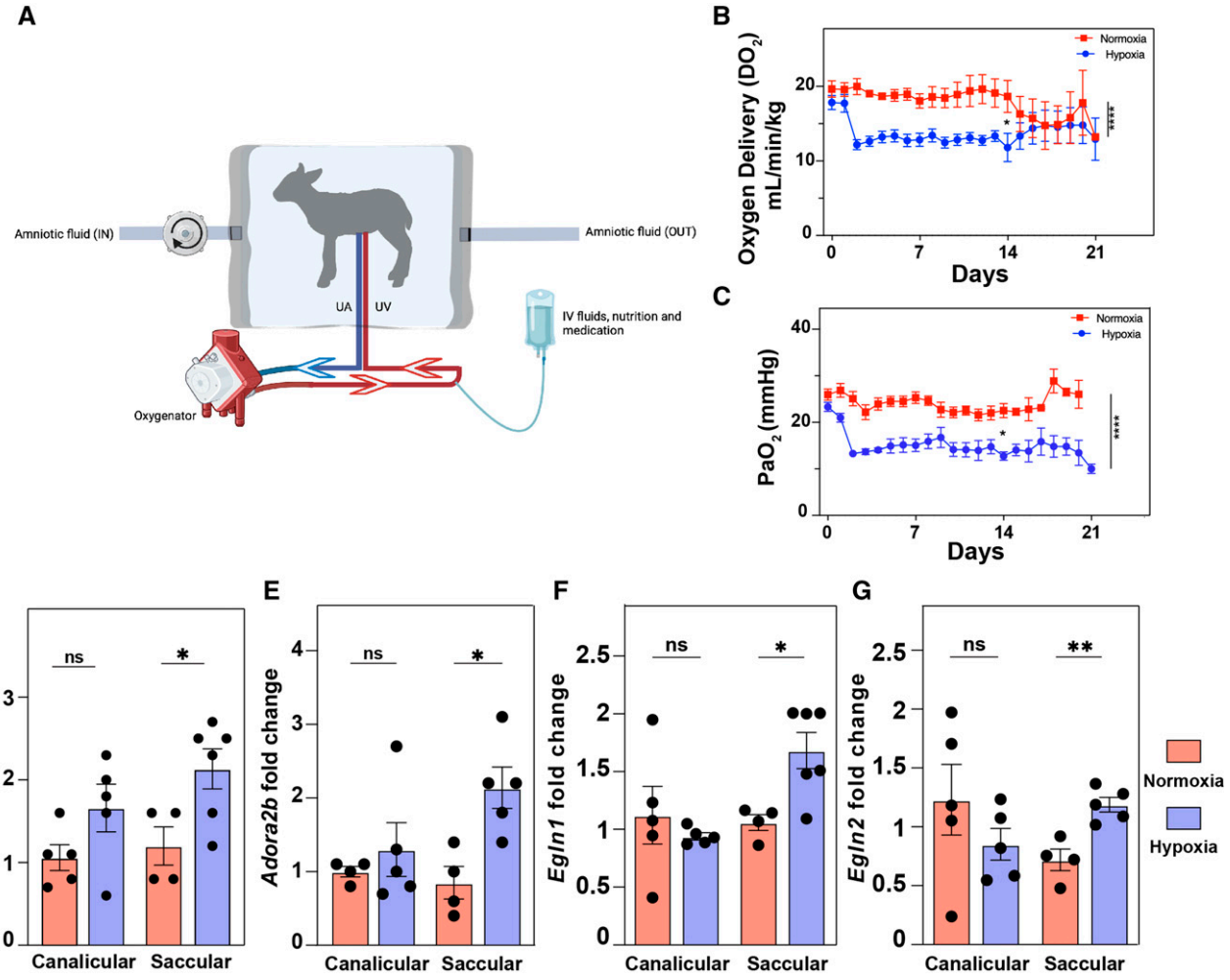

Figure 1. Hypoxia in the Extrauterine Environment for Neonatal Development (EXTEND) model. (*A*) EXTEND system diagram, including the closed fluid system with continuous exchange and the pumpless fetal oxygenation circulation. (*B*) Oxygen delivery. (*C*) Pa_{O_2}. (*D–G*) Quantitative PCR (qPCR) for *Vegfa* (vascular endothelial growth factor A) (*D*), *Adora2b* (adenosine A2B receptor) (*E*), *Egln1* (egl-9 homolog 1) (*F*), and *Egln2* (egl-9 homolog 2) (*G*). qPCR data are expressed as relative fold change compared with the canalicular normoxic group. $*P \leq 0.05$, $**P \leq 0.01$, and $****P \leq 0.0001$. In *B* and *C*, $n = 9$ and $n = 11$ sheep in the normoxia and hypoxia groups, respectively; in *D–G*, the number of sheep is represented by dots on the graphs. IV = intravenous; ns = not significant ($P > 0.05$); Pa_{O_2} = partial pressure of oxygen; UA = umbilical artery; UV = umbilical vein.

revealed increased combined cardiac output in hypoxic conditions compared with normoxic lambs in the canalicular group (Table 1). Despite increased combined cardiac output, the ratio of right ventricular to left ventricular cardiac output remained stable in all study groups. In terms of somatic growth, hypoxic animals showed a progressive decrease in animal weight, growth rate, and femur length over time, consistent with findings of IUGR (Table 1).

EXTEND-mediated Isolated Chronic Hypoxia Results in Loss of Endothelium

Hypoxia incites multiple signaling pathways with widespread implications on developing organs. As such, we analyzed gene expression of several hypoxia-associated genes by qPCR to confirm the EXTEND-derived hypoxic environment. Although analysis of hypoxia inducible factor 1α (*Hif1a*) and *Hif2a* revealed no change in gene expression during chronic hypoxia, there was a significant increase in *Hif3a* ($P = 0.009$ in the saccular stage; *see* Figures E1B–E1D). To further assess hypoxic effects in the lung, we examined direct HIF1A target genes important for lung development and injury responses, including *Vegfa* and the adenosine signaling components *Adora2b*, *Adk*, *Ada*, and *Nt5e* (24–26). Similar to previously published data, we saw statistically significant increases during the saccular stage in the HIF1A target genes *Vegfa* ($P = 0.04$) and *Adora2b* ($P = 0.01$) (Figure 1D and 1E) and appropriate data trends in increased or decreased adenosine signaling components (*see* Figures E1E–E1G). In addition, we observed an increase in mRNA expression of the EGL-9 gene family members targeted by HIFs (27) *Egln1* ($P = 0.02$) and *Egln2* ($P = 0.003$), during exposure to hypoxia in the saccular stage (Figures 1F and 1G).

Given that the major regulation of HIFs are at the protein level, we assessed HIF1A expression using western blotting in addition to IHC with antibodies for HIF1A and the pan-endothelial marker ERG (ETS-related gene) to delineate vasculature (Figures 2 and E2). By western blotting, HIF1A protein was significantly increased under hypoxic conditions during the saccular stage of lung development ($P = 0.049$) (Figures 2D and 2E). In addition, on IHC, HIF1A was increased in the ERG^+ endothelium, demonstrating cell-specific regulation of HIF1A ($P = 0.03$) (*see* Figures E2A–E2E). Interestingly, a target and important regulator of HIF1A protein stabilization, EGLN1 protein, was also increased with chronic hypoxia in the saccular stage ($P = 0.033$) (Figures 2D and 2F), consistent with a previously reported feedback mechanism between HIFs and EGLNs (28).

Chronic fetal hypoxia can cause impaired vascularization, which in turn causes delayed alveolarization (29). We assessed vascular remodeling by quantifying macrovessel count and microvessel EC number, neomuscularization of distal vessels, and percentage medial wall thickness (%MWT). Using double-fluorescent IHC with antibodies to von Willebrand factor (VWF) and ACTA2, we noted that the total number of macroscopic vessels significantly decreased in hypoxic conditions in the saccular group ($P = 0.03$; Figures 3A–3E). In addition, the analysis of microvasculature using a pan-endothelial antibody to ERG combined with anti-VWF antibody to exclude macrovasculature showed a significant reduction in ERG^+ microvascular ECs under hypoxic conditions to the canalicular ($P = 0.02$) and saccular ($P = 0.04$) stages, supporting loss of endothelium in hypoxia (Figures 3F–3J).

We also assessed %MWT of the total vessel diameter in vessels ranging in size from 20 to 200 μm (Figure 4). Overall, %MWT in the canalicular animal group was similar in both hypoxic and normoxic conditions ($P = 0.97$) (Figures 4A–4D). However, in the saccular animal group, %MWT in all vessels combined was modestly increased in hypoxic lambs ($P = 0.03$) (Figures 4E–4G). However, in individual vessel diameter groups, there was no statistically significant change in medial wall thickness (Figure 4H).

Neomuscularization of peripheral vessels was analyzed in our cohort. Fully muscularized vessels (Figures 4I–4N) were similar in both hypoxic and normoxic conditions in both canalicular and saccular

Table 1. Animal Vital Signs and Echocardiographic Parameters on Extrauterine Environment for Neonatal Development

	Canalicular Group			Saccular Group		
	Normoxia ($n = 4$)	Hypoxia ($n = 5$)	*P* Value	Normoxia ($n = 4$)	Hypoxia ($n = 6$)	*P* Value
Echocardiographic parameters						
CCO, ml/kg/min	530 ± 35.8	655 ± 28.7	**0.03**	543.5 ± 20.6	609.6 ± 21.4	0.07
RV output, ml/kg/min	336.6 ± 17.4	381.8 ± 35	0.26	350.4 ± 25.9	387 ± 14.6	0.22
LV output, ml/kg/min	193.4 ± 15.5	264.7 ± 15.7	**0.02**	191.6 ± 9.6	222.6 ± 12.8	0.11
RV:LV output ratio	1.8 ± 0.3	1.5 ± 0.1	0.15	1.9 ± 0.2	1.8 ± 0.1	0.6
DA flow, ml/kg/min	155.1 ± 25.3	193.3 ± 18.8	0.25	193.5 ± 14.5	216.4 ± 12.3	0.27
DA flow:RV output ratio	0.5 ± 0.1	0.5 ± 0.04	0.66	0.57 ± 0.03	0.57 ± 0.04	0.87
Growth parameters						
Growth rate, g/kg/J	91.4 ± 20.7	39.2 ± 8.1	**0.047**	33 ± 4.2*	19.5 ± 2.4	**0.02**
Femur length, cm	7.5 ± 0.08	7.2 ± 0.3	0.33	8.4 ± 0.4	7.3 ± 0.3	**0.047**
Weight, fold change	0.5 ± 0.08†	0.27 ± 0.06	**0.03**	0.8 ± 0.2	0.4 ± 0.04†	**0.03**
Lung weight:animal weight	34.7 ± 6.3	34 ± 4	0.93	29.4 ± 4.5	33.7 ± 3.5	0.47
Lung volume:animal weight	21.5 ± 4.3	23.9 ± 2.8	0.64	19.3 ± 3.6	20.4 ± 2	0.79

Definition of abbreviations: CCO = combined cardiac output; DA = ductus arteriosus; LV = left ventricle; RV = right ventricular.
Data are expressed as mean ± SEM.
Bolded values indicate data reaching statistical significance ($P < 0.05$).
*One animal in the saccular group was excluded for growth rate because of severe ascites at the time of necropsy.
†One animal in the canalicular normoxic group and one in the saccular hypoxic group were excluded for growth rate because of severe ascites at the time of necropsy.

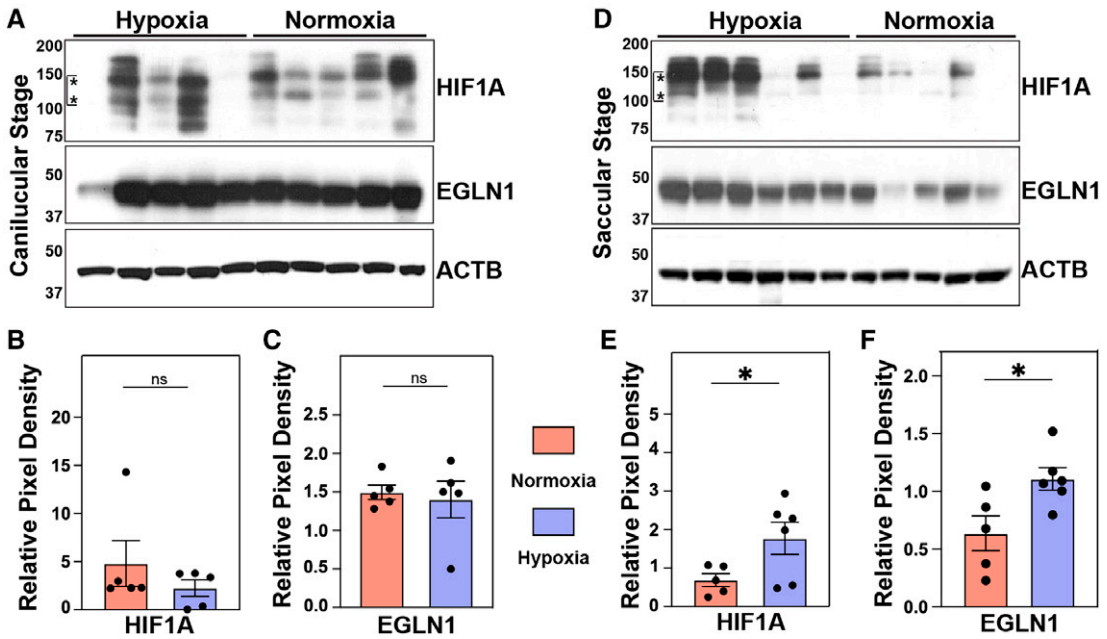

Figure 2. Hypoxia-related protein regulation after chronic hypoxia on EXTEND. (*A*) Hypoxia inducing factor 1A (HIF1A), egl-9 homolog 1 (EGLN1) and beta-actin expression (ACTB) in the canalicular group with quantification of (*B*) HIF1A and (*C*) EGLN1. Bracket with asterisks represents HIF1A. (*D*) HIF1A, EGLN1 and ACTB in the saccular group with quantification of (*E*) HIF1A and (*F*) EGLN1. Bracket with asterisks represents HIF1A. Statistical significance is expressed by ns= $P > 0.05$, *= $P \leq 0.05$. The number of sheep for each group (n) is represented on the graph.

animal groups. Nonmuscularized vessels trended lower in both canalicular and saccular group in hypoxic conditions. In parallel, partially muscularized vessels significantly increased ($P = 0.03$; Figure 4K) under hypoxic conditions in the canalicular group and showed a similar trend in the saccular group under hypoxic condition (Figure 4N).

Isolated Chronic Hypoxia Alters Lung Structure

Exposure to a hypoxic environment resulted in deficiencies in somatic growth. Thus, we asked whether isolated hypoxia significantly reduced the growth of fetal lung weight and lung volume as indirect markers of lung size. There was no difference in the ratio of lung weight or volume to body weight, suggesting a more global growth defect and consistent with previous data (Table 1) (8, 30, 31).

Oxygen tension also plays a significant role in prenatal and postnatal lung saccule and alveolar formation. Using the mean linear intercept to determine distal airway size and septal volume analyses, we assessed the ultrastructure of the distal lung to analyze the effects of chronic isolated hypoxia on airspace formation (Figures 5A–5F). By measuring the mean linear intercept, distal airspace size increased over time in hypoxic conditions in the saccular group ($P = 0.047$) (Figure 5C). In addition, septal volume was significantly decreased in the canalicular group under hypoxic conditions on EXTEND ($P = 0.02$) (Figure 5F). Despite this, lung cellularity as measured by DAPI cell count showed no difference between hypoxic and normoxic conditions in the canalicular group ($P = 0.4$) or in the saccular group ($P = 0.2$) (*see* Figure E3A).

Isolated Chronic Hypoxia Delays Surfactant Production

Pulmonary surfactant production plays an important role in lung development by reducing alveolar surface tension required for adequate transition to air breathing. First, we examined both SFTPB (surfactant protein B) and SFTPC expression using western blotting for surfactant proteins in whole-lung lysates. Notably, there was a significant decrease in mature SFTPB in hypoxic conditions during the canalicular stage ($P = 0.01$), with a similar trend in the saccular group ($P = 0.17$; Figures 6A and 6B). Similarly, processed, mature SFTPC was reduced under hypoxic conditions in the canalicular group ($P = 0.01$), with a similar trend in the saccular group ($P = 0.69$) (Figures 6C and 6D). However, assessment of pro-SFTPC showed no change in protein expression at any duration of hypoxia. To determine whether this loss was a result of affected translation, transcription, or processing, we performed qPCR for *Sftpb* and *Sftpc* and the surfactant processing genes *Abca3* and *Lamp3*. Although almost all transcripts for surfactant and surfactant processing genes trended downward with hypoxia, there was no statistical significance (*see* Figures E4A–E4D).

We further characterized whether loss of surfactant protein production could be due to a decrease in AT2 cells. Using IHC for SFTPB, we identified AT2 cells and quantified them in relation to the total number of cells. Qualitatively, there appeared to be a marked reduction in the number of AT2 cells under hypoxic conditions during both the canalicular ($P = 0.003$) and saccular ($P = 0.03$) stages (Figures 7A, 7B, 7D, and 7E). These findings were confirmed by quantifying the total number of AT2 cells (Figures 7C and 7F). To determine if these losses were associated with lung cortisol changes, a hormone that can promote AT2 cell maturation and surfactant production (32), lung cortisol quantification was performed and demonstrated no change in both the hypoxic canalicular ($P = 0.8$) and saccular ($P = 0.7$) groups (*see* Figure E4E).

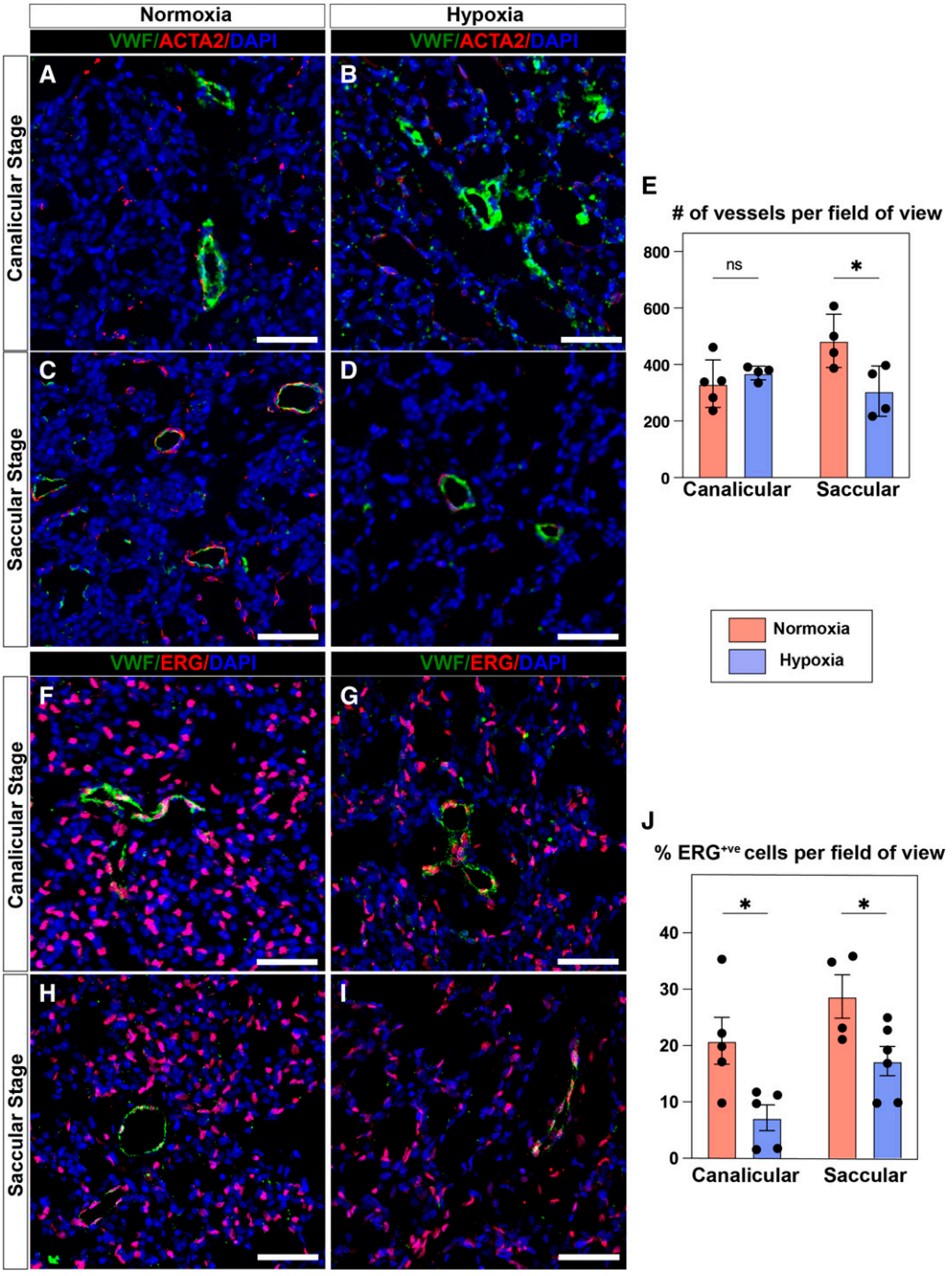

Figure 3. EXTEND-mediated chronic hypoxia effects on the endothelium. (*A–E*) Quantification of macrovessel number. (*A* and *B*) Canalicular stage lung tissue sections stained for anti–von Willebrand factor (VWF) and antiACTA2 in normoxic (*A*) and hypoxic (*B*) conditions. (*C* and *D*) Saccular stage lung tissue sections stained for VWF and ACTA2 in normoxic (*C*) and hypoxic (*D*) conditions. (*E*) Quantification of the number of macroscopic vessels. (*F–J*) Quantification of microvascular endothelial cell (EC) number. (*F* and *G*) Canalicular stage lung tissue sections stained for nuclear pan-endothelial markers ERG (ETS-related gene) and VWF in normoxic (*F*) and hypoxic (*G*) conditions. (*H* and *I*) Saccular stage lung tissue sections stained for ERG and VWF in normoxic (*H*) and hypoxic (*I*) conditions. (*J*) Microvascular EC quantification. $^{*}P \leq 0.05$. The number of sheep for each group is represented on the graphs. Scale bars, 50 μm.

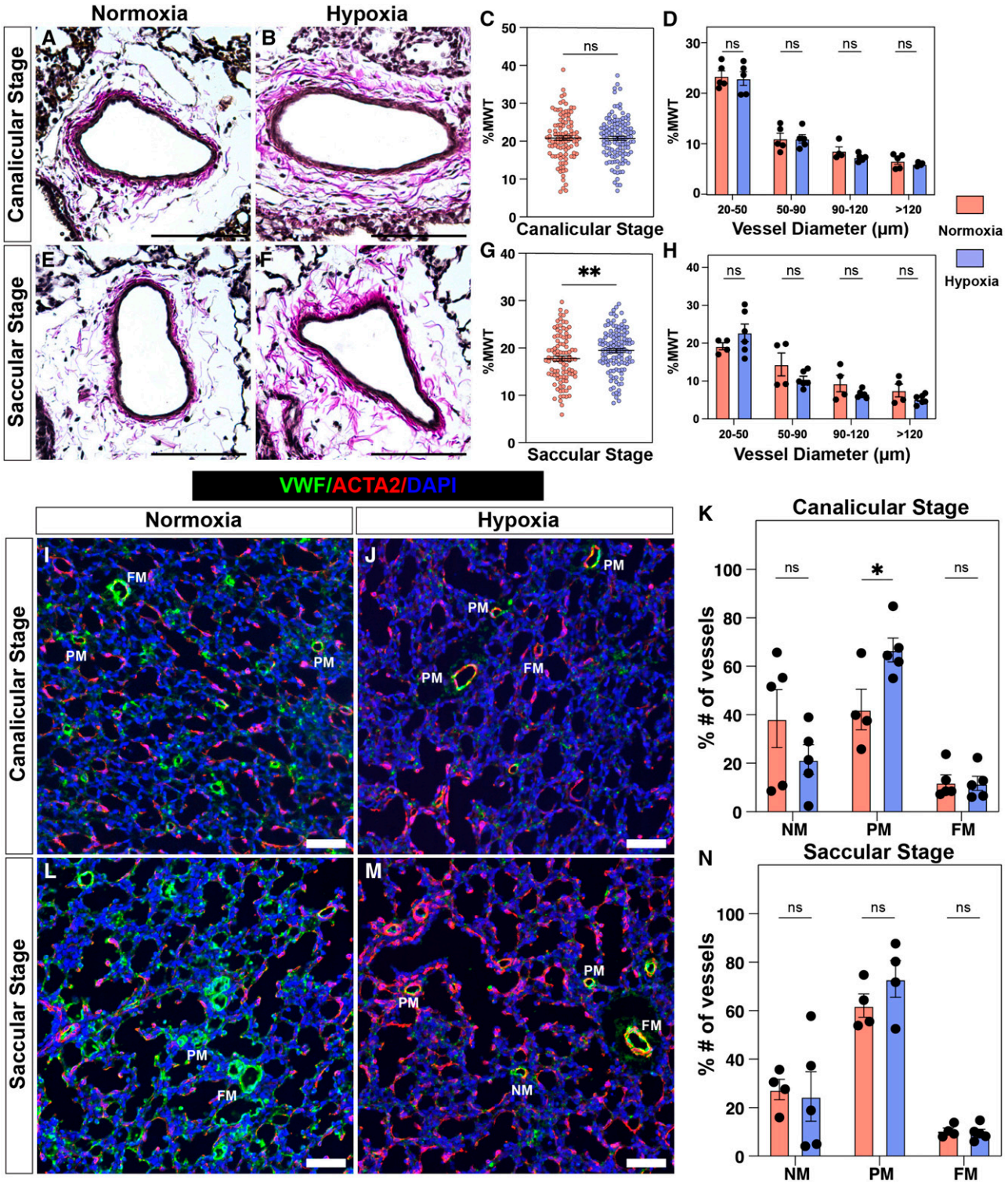

Figure 4. Aberrant vascular remodeling induced by chronic hypoxia in EXTEND. (*A–H*) %MWT of arterioles with external vessel diameters between 20 and 200 μm. (*A–D*) Verhoeff's elastin stain to delineate the medial wall in normoxic (*A*) and hypoxic (*B*) conditions in the canalicular stage, with quantification of all vessel sizes combined (*C*) versus quantification by vessel size subdivision (*D*). (*E–H*) Verhoeff's elastin stain to delineate the medial wall in normoxic (*E*) and hypoxic (*F*) conditions in the saccular stage, with quantification of all vessel sizes combined (*G*) versus quantification by vessel size subdivision (*H*). (*I–N*) Quantification of neomuscularization of peripheral vessels. (*I–K*) VWF and ACTA2 staining for endothelium and smooth muscle in normoxic (*I*) and hypoxic (*J*) conditions in the canalicular stage, with quantification of percentage

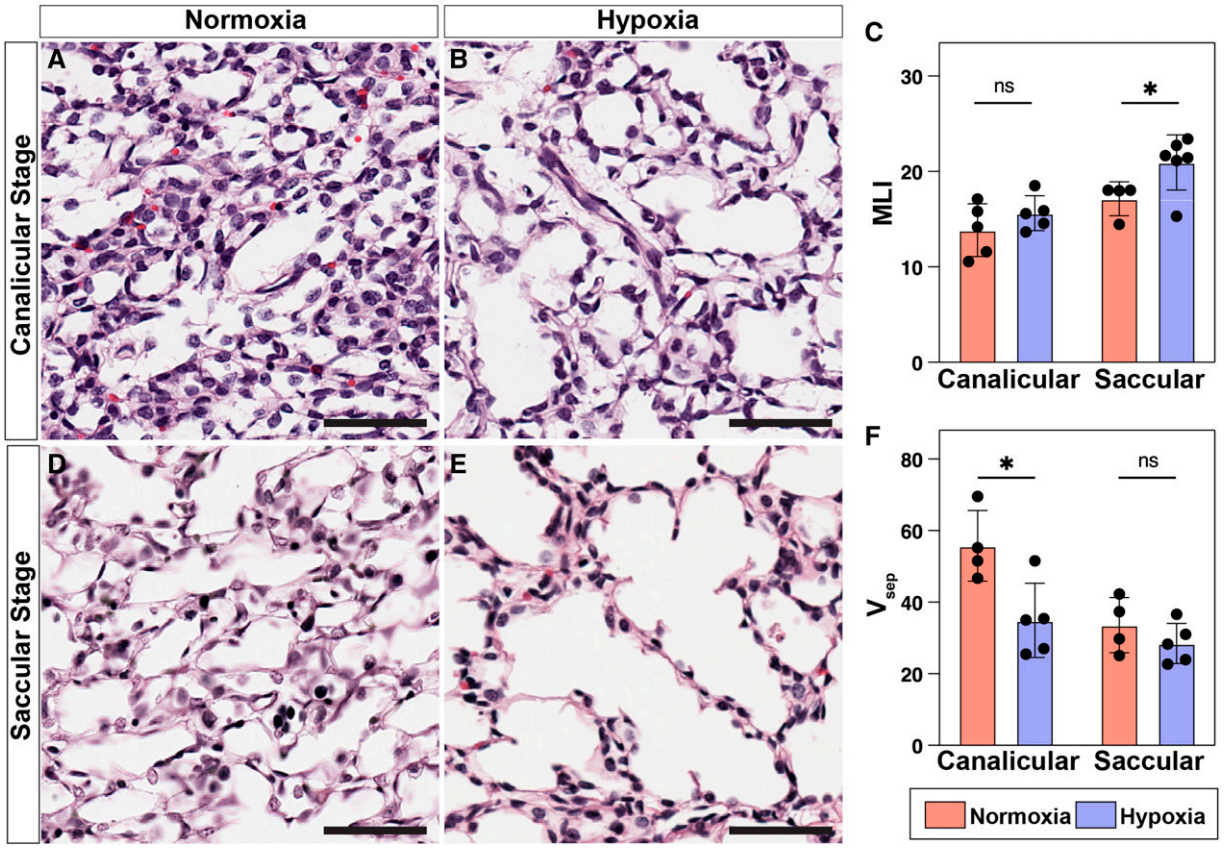

Figure 5. Chronic hypoxia in EXTEND affects distal airway growth and morphogenesis. (*A–D*) Canalicular (*A* and *B*) and saccular (*C* and *D*) stage lung sections stained with hematoxylin and eosin in normoxic (*A* and *C*) and hypoxic (*B* and *D*) conditions. (*E* and *F*) Measurements of MLI (*E*) and V_{sep} (*F*). *$P \leq 0.05$. The number of sheep for each group is represented on the graphs. Scale bars, 50 μm. MLI = mean linear intercept; V_{sep} = absolute volume of alveolar septa.

Discussion

Previously, EXTEND has been shown to support premature lamb development and growth for up to four weeks in physiologic conditions, supporting the ability to safely manipulate environment variables for additional studies. With EXTEND, we have demonstrated that isolated fetal hypoxia disrupts normal lung development in lambs, resulting in distal airway simplification, aberrant vascular remodeling, and delayed surfactant maturation. To our knowledge, this study is the first to investigate the developmental effects of isolated fetal hypoxia on lung development independent of a maternal environment. Similar to previous studies assessing this established model on cardiac and brain development, these findings are important for not only outcomes associated with etiologies of isolated fetal hypoxia but also hypoxia associated with mixing physiology lesions in congenital heart disease (19, 21–23).

An essential challenge in investigating the consequences of severe fetal hypoxia is the reliability of the animal model used. The most commonly used method to reproduce fetal hypoxia is by interfering with uteroplacental blood flow (carunclectomy, placental embolization, uterine blood flow restriction, single umbilical artery ligation, and compression of the umbilical cord). However, these techniques also restrict blood flow and thus nutrient supply, which is more closely related to IUGR models than fetal hypoxia itself (6). Other animal models induce maternal hypoxia by either using natural hypobaric hypoxia experienced at high altitude or using isobaric hypoxic chambers. However, the maternal response to hypoxia can affect fetal response, which restricts the accurate analysis of the effects of fetal hypoxia (33). This study produces severe fetal hypoxia by maintaining controlled isolated chronic fetal hypoxia for an extended period of gestation without maternal impact.

Fetal cardiovascular response to acute fetal hypoxia has been well described (6, 33–35). In contrast, our understanding of

Figure 4. (*Continued*). nonmuscularized (NM), partially muscularized (PM), and fully muscularized (FM) peripheral vessels (*K*). (*L–N*) VWF and ACTA2 staining of lung tissue sections in normoxic (*L*) and hypoxic (*M*) conditions in the canalicular stage, with quantification of percentage NM, PM, and FM peripheral vessels (*N*). *$P \leq 0.05$ and **$P \leq 0.01$. In *C* and *G*, $n = 10$ and $n = 11$ sheep in the normoxia and hypoxia groups, respectively; in *D*, *H*, *K*, *N*, the number of sheep is represented by dots on the graphs. Scale bars, 50 μm. %MWT = percentage medial wall thickness.

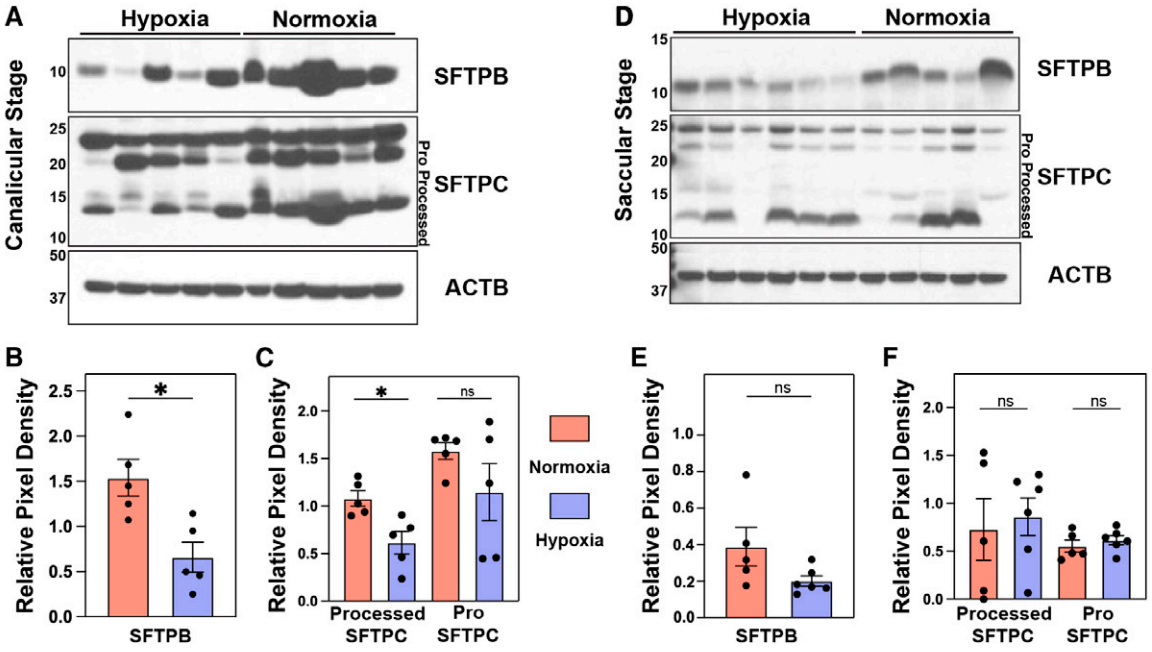

Figure 6. Diminished surfactant protein metabolism after chronic hypoxia on EXTEND. (*A*) Mature surfactant protein B (SFTPB), pro-surfactant protein C (pro-SFTPC), processed and mature SFTPC, and beta-actin expression (ACTB) in the canalicular group with quantification of (*B*) SFTPB and (*C*) processed SFTPC, and pro-SFTPC. (*D*) SFTPB, pro-SFTPC, processed and mature SFTPC, and ACTB (right panels) in the saccular group with quantification of (*E*) SFTPC and (*F*) processed SFTPC and pro-SFTPC. Statistical significance is expressed by ns= $P > 0.05$ and *= $P \leq 0.05$. The number of sheep for each group (n) is represented on the graph.

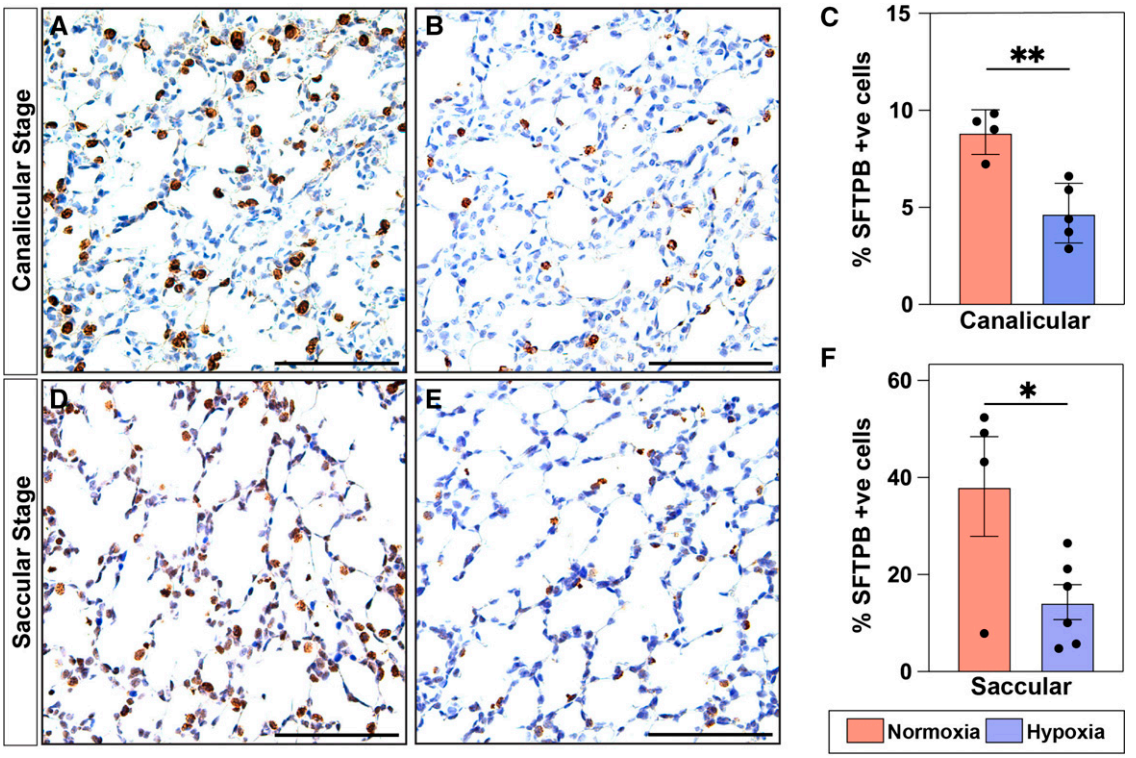

Figure 7. Alveolar type 2 (AT2) cell reduction after chronic hypoxia on EXTEND. (*A* and *B*) IHC for SFTPB to identify AT2 cells for cell number quantification in normoxic (*A*) and hypoxic (*B*) conditions in the canalicular group. (*C*) AT2 cell quantification in the canalicular group. (*D* and *E*) IHC for SFTPB to identify AT2 cells for cell number quantification in normoxic (*D*) and hypoxic (*E*) conditions in the saccular group. (*F*) AT2 cell quantification in the saccular group. *$P \leq 0.05$ and **$P \leq 0.01$. The number of sheep for each group is represented on the graphs. Scale bars, 50 μm.

the mechanisms that mediate the fetal hemodynamic response to chronic fetal hypoxia is incomplete. Similar to acute fetal hypoxia, it is widely believed that chronically hypoxic fetuses experience a redistribution of the blood flow away from the periphery, which contributes significantly to the commonly observed growth restriction in hypoxic conditions (6, 33–35). In our cohort, animal growth, defined by weight fold change, growth rate, and femur length, was significantly reduced in hypoxic conditions, as expected.

Hemodynamically, acute fetal hypoxia is responsible for decreased heart rate (36) and peripheral vasoconstriction. However, response to hypoxia has been believed to be blunted in chronic setting of fetal hypoxia compared with acute episodes (37). Several studies of chronic fetal hypoxia showed no differences in heart rate and blood pressure during prolonged hypoxia (33, 35). In our cohort, fetal hypoxia was maintained for up to 21 days. Animal vitals (heart rate, circuit blood flow, and circuit mean arterial pressures) were similar in both study groups.

At the cellular level, fetal hypoxia triggers the activation of the hypoxia signaling cascade regulated by the HIFs. This paradigm was also present in our results: HIF1A was increased under hypoxic conditions in the saccular stage. Importantly, we also demonstrated endothelium-specific regulation of HIF1A in our model, and we observed statistically significant increases and trends for several direct target genes of HIF1A, including *Vegfa* and the adenosine signaling component *Adora2b* (24). Both VEGFA and adenosine signaling have significant implications in not only vascular development and abnormal remodeling but also severe airspace defects in development and developmental injury (25, 26). Our study also confirmed increased mRNA and protein expression of some of the EGL-9 family members that are associated with chronic fetal hypoxia and potential transcriptional targets of HIF proteins (38). These findings are consistent with induced pulmonary hypoxia signaling pathways in chronic hypoxia on EXTEND.

During fetal development, the pulmonary circulation exhibits elevated vasomotor tone due to muscularization, causing increased pulmonary vascular resistance. Severe fetal hypoxia has been associated with failed transition of the fetal circulation at birth, leading to PPHN (37, 39). Factors such as inadequate vascular relaxation, excessive muscularization (increased vascular wall thickness and distal extension of muscle in vessels normally devoid of muscularization), and reduced vascular density contribute to PPHN (39–41). These findings have been demonstrated in previous studies done on lambs born at high altitude, indicating a PPHN-like disease (42). In our isolated hypoxia model, lambs showed only modest aberrant vascular remodeling, which may reflect a shorter period of exposure to hypoxia. Alternatively, the lower severity of vascular remodeling in our study may suggest that changes in fetal pulmonary blood flow play an additional role in remodeling. Prior studies of fetal hypoxia with more severe remodeling may reflect both flow and hypoxia. Importantly, most patients with cyanotic/mixed physiology lesions of congenital heart disease do not exhibit PPHN associated with vascular remodeling, suggesting that severe vascular remodeling is compounded by both flow and oxygen tension (43, 44). Furthermore, persistent cyanosis after delivery or surgery may indicate a need to explore findings of delayed maturation of the distal lung.

The effects of hypoxia on lung development depend on the timing and duration of hypoxia. In our model, hypoxia was induced during midcanalicular stage of lung development, which is when gas exchange is possible (~22 wk of human gestation). Studies on severe chronic fetal hypoxia induced at similar gestational ages showed preserved lung growth on the basis of the ratio of lung weight to body weight (8, 31). However, lamb models inducing hypoxia during the early canalicular stage exhibited an increased proportion of airspace parenchymal volume and reduced tissue elements in this gas-exchange region (31). In contrast, hypoxia induced during the saccular stage resulted in fewer alveoli, thicker intraalveolar septa, and persistent thickening of the basement membrane (45). Another study conducted on pregnant rats exposed to hypoxia throughout pregnancy revealed decreased septation, reduced alveoli, and increased volume of alveolar saccules. In our isolated chronic fetal hypoxia model, the results showed a simplification of the distal airways, as seen in several other hypoxia animal models (31, 45).

Another important aspect of lung development for adequate transition to air breathing is pulmonary surfactant, which reduces lung surface tension at the air–liquid interface and prevents alveolar collapse. Surfactant maturation occurs during the saccular stage of lung development, corresponding to a 25-week gestation human fetus or a 120-day gestation lamb fetus (46). The effect of fetal hypoxia on surfactant production has been shown to be dependent on the duration and timing of exposure (7, 8). Specifically, chronic hypoxia induced later in gestation resulted in increased surfactant protein production (18, 47), while exposure to chronic hypoxia earlier in pregnancy led to decreased surfactant protein regulation (8, 38, 48). In our study, direct induction of chronic fetal hypoxia in the midcanalicular stage caused reductions in SFTPB and SFTPC total protein expression, likely most consistent with a reduction in the number of AT2 cells. Previous research indicated a correlation between decreased AT2 cells and lower surfactant production, as evidenced by reduced proliferation markers (38). However, contrary to expectations, sheep models experiencing chronic fetal hypoxia show no significant decline in AT2 cell density, suggesting a molecular basis for the variation in surfactant protein gene expression (18, 48). Yet comparing these findings with those of other groups is complex because of the unique nature of the EXTEND hypoxia model, which presents isolated chronic fetal hypoxia. Moreover, epithelial cell numbers in developing lambs vary significantly with gestational age. Therefore, it is crucial to compare studies involving lambs at the same gestational age, subjected to similar hypoxia timing, to draw accurate conclusions. This discrepancy underscores the critical role of the chosen model in describing severe fetal hypoxia. Interestingly, there was no significant effect of chronic fetal hypoxia on lung cortisol concentrations, consistent with previous findings (18). These data suggest that delayed surfactant maturation without altered cortisol signaling was caused by isolated chronic fetal hypoxia.

Limitations

Our animal model showed some variability in the outcomes, as the response to the new environment could have slightly differed among animals maintained on EXTEND for up to 21 days. In addition, our study was limited to small sample sizes because of the resource-intensive nature of maintaining fetal lambs on EXTEND. A preexperimental power analysis for this study is difficult, as it is a new model in which effect size would be

difficult to calculate because of the novelty/unknown effect. In addition, the model was costly and labor intensive given U.S. Food and Drug Administration regulations guiding its potential use in humans. A *post hoc* power analysis was performed and showed that some of the experiments in the present study did not reach significant numbers, indicating an inability to address whether sex differences exist (*see* Table E4). However, additional studies involving increased animal numbers with equal numbers of male and female preterm lambs will be key to addressing this important issue.

The maximum duration of hypoxia was limited to 21 days for technical reasons, potentially underestimating the complications of chronic fetal hypoxia in human pathology with prolonged fetal hypoxia. Similarly, the timing of hypoxia induction differs from some of the previously published research inducing chronic fetal hypoxia earlier or later in the pregnancy. Comparing the EXTEND model with previously published fetal hypoxia models is challenging because of its unique isolated chronic fetal hypoxia. Therefore, interpreting comparisons with other IUGR models requires caution. In addition, lung development can be influenced by various factors, such as amniotic fluid pressure, head and neck position, modified pulmonary blood flow, and others. In our animal model, both study groups were treated similarly to minimize additional confounding factors.

Last, the previously published (14) methods used to quantify lung structure made use of paraffin-embedded tissue, and despite showing increased reproducibility compared with manual counting techniques, it did not include all the components of design-based stereology. Design-based stereology is the standard for quantification, as it eliminates bias using three-dimensional imaging, improves the accuracy of cell type localization, and allows more rigorous assessment of volume density measurements (49, 50). Nevertheless, despite reduced model variability, reduced sample size, duration of hypoxia, and possible confounding factors, we were able to identify significant differences between groups, with clear molecular and histological impact of chronic fetal hypoxia on lung development.

Conclusions

We used a previously described model of chronic isolated fetal hypoxia for lung development analysis. Animals maintained in hypoxic conditions on EXTEND for prolonged periods of time showed significant growth restriction and increased combined cardiac output at daily cardiac ultrasound. Lungs showed arrested development with distal airway simplification. Vascular remodeling was present in hypoxic conditions, including mildly increased vessel wall thickness, some increased muscularization, and reduced macrovessel count and microvessel EC number. In parallel, SFTPB and SFTPC were reduced, and lungs exhibited a decrease in AT2 cells. These findings provide clarity regarding the effects of hypoxia on lung development and demonstrate that isolated hypoxia directly affects distal airway development. Further studies on our isolated fetal hypoxia animal model are necessary to assess vascular contractility, further mechanisms of vascular remodeling, distal airway growth, and surfactant lipid metabolism to depict a clearer picture of the impact of hypoxia on lung development. ■

Author disclosures are available with the text of this article at www.atsjournals.org.

Acknowledgment: The authors thank the entire lamb team that assisted with these studies, including but not limited to Copeland Rouse, Ryan Benjamin, Samantha Plante, Madison Ehler, Jonathan Chang, and Abby Larson. Special thanks to Aaron Weilerstein for his role with animal maintenance, husbandry, and surgery anesthesia.

References

1. Hutter D, Kingdom J, Jaeggi E. Causes and mechanisms of intrauterine hypoxia and its impact on the fetal cardiovascular system: a review. *Int J Pediatr* 2010;2010:401323.
2. Chen EY, Fujinaga M, Giaccia AJ. Hypoxic microenvironment within an embryo induces apoptosis and is essential for proper morphological development. *Teratology* 1999;60:215–225.
3. van Tuyl M, Liu J, Wang J, Kuliszewski M, Tibboel D, Post M. Role of oxygen and vascular development in epithelial branching morphogenesis of the developing mouse lung. *Am J Physiol Lung Cell Mol Physiol* 2005; 288:L167–L178.
4. Rueda-Clausen CF, Morton JS, Davidge ST. Effects of hypoxia-induced intrauterine growth restriction on cardiopulmonary structure and function during adulthood. *Cardiovasc Res* 2009;81:713–722.
5. Anderson RN, Smith BL. Deaths: leading causes for 2002. *Natl Vital Stat Rep* 2005;53:1–89.
6. Morrison JL. Sheep models of intrauterine growth restriction: fetal adaptations and consequences. *Clin Exp Pharmacol Physiol* 2008;35: 730–743.
7. McGillick EV, Orgeig S, Williams MT, Morrison JL. Risk of respiratory distress syndrome and efficacy of glucocorticoids: are they the same in the normally grown and growth-restricted infant? *Reprod Sci* 2016;23: 1459–1472.
8. Orgeig S, Crittenden TA, Marchant C, McMillen IC, Morrison JL. Intrauterine growth restriction delays surfactant protein maturation in the sheep fetus. *Am J Physiol Lung Cell Mol Physiol* 2010;298:L575–L583.
9. Partridge EA, Davey MG, Hornick MA, McGovern PE, Mejaddam AY, Vrecenak JD, *et al.* An extra-uterine system to physiologically support the extreme premature lamb. *Nat Commun* 2017;8:15112.
10. De Bie FR, Davey MG, Larson AC, Deprest J, Flake AW. Artificial placenta and womb technology: past, current, and future challenges towards clinical translation. *Prenat Diagn* 2021;41:145–158.
11. Ozawa K, Davey M, Tian Z, Hornick M, Mejaddam A, McGovern P, *et al.* Fetal echocardiographic assessment of cardiovascular impact of prolonged support on Extrauterine Environment for Neonatal Development (EXTEND) system. *Ultrasound Obstet Gynecol* 2020;55: 516–522.
12. Peers de Nieuwburgh M, Dave A, Khan SA, Ngo M, Hayes KB, Slipenchuk M, *et al.* Assessment of extremely premature lambs supported by the Extrauterine Environment for Neonatal Development (EXTEND). *Pediatr Res* [online ahead of print] 4 Jun 2024; DOI: 10.1038/s41390-024-03287-0.
13. Sun L, Macgowan CK, Sled JG, Yoo S-J, Manlhiot C, Porayette P, *et al.* Reduced fetal cerebral oxygen consumption is associated with smaller brain size in fetuses with congenital heart disease. *Circulation* 2015; 131:1313–1323.
14. Salaets T, Tack B, Gie A, Pavie B, Sindhwani N, Jimenez J, *et al.* A semi-automated method for unbiased alveolar morphometry: validation in a bronchopulmonary dysplasia model. *PLoS One* 2020;15:e0239562.
15. McGillick EV, Orgeig S, Morrison JL. Regulation of lung maturation by prolyl hydroxylase domain inhibition in the lung of the normally grown and placentally restricted fetus in late gestation. *Am J Physiol Regul Integr Comp Physiol* 2016;310:R1226–R1243.
16. McGillick EV, Orgeig S, McMillen IC, Morrison JL. The fetal sheep lung does not respond to cortisol infusion during the late canalicular phase of development. *Physiol Rep* 2013;1:e00130.
17. Passmore M, Nataatmadja M, Fraser JF. Selection of reference genes for normalisation of real-time RT-PCR in brain-stem death injury in *Ovis aries*. *BMC Mol Biol* 2009;10:72–78.

18. McGillick EV, Orgeig S, Allison BJ, Brain KL, Niu Y, Itani N, *et al.* Maternal chronic hypoxia increases expression of genes regulating lung liquid movement and surfactant maturation in male fetuses in late gestation. *J Physiol* 2017;595:4329–4350.
19. Lawrence KM, McGovern PE, Mejaddam A, Rossidis AC, Baumgarten H, Kim A, *et al.* Chronic intrauterine hypoxia alters neurodevelopment in fetal sheep. *J Thorac Cardiovasc Surg* 2019;157:1982–1991.
20. Rossidis AC, Baumgarten HD, Lawrence KM, McGovern PE, Mejaddam AY, Li H, *et al.* Chronically hypoxic fetal lambs supported by an extra-uterine device exhibit mitochondrial dysfunction and elevations of hypoxia inducible factor 1-alpha. *Fetal Diagn Ther* 2019;45: 176–183.
21. McGovern PE, Lawrence K, Baumgarten H, Rossidis AC, Mejaddam AY, Licht DJ, *et al. Ex utero* extracorporeal support as a model for fetal hypoxia and brain dysmaturity. *Ann Thorac Surg* 2020;109:810–819.
22. Lawrence KM, Hennessy-Strahs S, McGovern PE, Mejaddam AY, Rossidis AC, Baumgarten HD, *et al.* Fetal hypoxemia causes abnormal myocardial development in a preterm *ex utero* fetal ovine model. *JCI Insight* 2018;3:3.
23. Lawrence KM, McGovern PE, Mejaddam A, Rossidis AC, Baumgarten H, Kim AG, *et al.* Prenatal hypoxemia alters microglial morphology in fetal sheep. *J Thorac Cardiovasc Surg* 2020;159:270–277.
24. Poth JM, Brodsky K, Ehrentraut H, Grenz A, Eltzschig HK. Transcriptional control of adenosine signaling by hypoxia-inducible transcription factors during ischemic or inflammatory disease. *J Mol Med (Berl)* 2013;91: 183–193.
25. Li H, Karmouty-Quintana H, Chen N-Y, Mills T, Molina J, Blackburn MR, *et al.* Loss of CD73-mediated extracellular adenosine production exacerbates inflammation and abnormal alveolar development in newborn mice exposed to prolonged hyperoxia. *Pediatr Res* 2017;82: 1039–1047.
26. Banerjee SK, Young HW, Barczak A, Erle DJ, Blackburn MR. Abnormal alveolar development associated with elevated adenine nucleosides. *Am J Respir Cell Mol Biol* 2004;30:38–50.
27. Metzen E, Stiehl DP, Doege K, Marxsen JH, Hellwig-Bürgel T, Jelkmann W. Regulation of the prolyl hydroxylase domain protein 2 (phd2/egln-1) gene: identification of a functional hypoxia-responsive element. *Biochem J* 2005;387:711–717.
28. Ginouves A, Ilc K, Macías N, Pouysségur J, Berra E. PHDs overactivation during chronic hypoxia "desensitizes" HIFα and protects cells from necrosis. *Proc Natl Acad Sci* 2008;105:4745–4750.
29. Jakkula M, Le Cras TD, Gebb S, Hirth KP, Tuder RM, Voelkel NF, *et al.* Inhibition of angiogenesis decreases alveolarization in the developing rat lung. *Am J Physiol Lung Cell Mol Physiol* 2000;279:L600–L607.
30. Rees S, Ng J, Dickson K, Nicholas T, Harding R. Growth retardation and the development of the respiratory system in fetal sheep. *Early Hum Dev* 1991;26:13–27.
31. Lipsett J, Tamblyn M, Madigan K, Roberts P, Cool JC, Runciman SI, *et al.* Restricted fetal growth and lung development: a morphometric analysis of pulmonary structure. *Pediatr Pulmonol* 2006;41:1138–1145.
32. Bolt RJ, Van Weissenbruch M, Lafeber H, Delemarre-Van De Waal H. Glucocorticoids and lung development in the fetus and preterm infant. *Pediatr Pulmonol* 2001;32:76–91.
33. Allison B, Brain K, Niu Y, Kane A, Herrera E, Thakor A, *et al.* Fetal in vivo continuous cardiovascular function during chronic hypoxia. *J Physiol* 2016;594:1247–1264.
34. Gardner DS, Giussani DA, Fowden AL. Hindlimb glucose and lactate metabolism during umbilical cord compression and acute hypoxemia in the late-gestation ovine fetus. *Am J Physiol Regul Integr Comp Physiol* 2003;284:R954–R964.
35. Poudel R, McMillen IC, Dunn SL, Zhang S, Morrison JL. Impact of chronic hypoxemia on blood flow to the brain, heart, and adrenal gland in the late-gestation IUGR sheep fetus. *Am J Physiol Regul Integr Comp Physiol* 2015;308:R151–R162.
36. Cohn HE, Sacks EJ, Heymann MA, Rudolph AM. Cardiovascular responses to hypoxemia and acidemia in fetal lambs. *Am J Obstet Gynecol* 1974;120:817–824.
37. Herrera EA, Rojas RT, Krause BJ, Ebensperger G, Reyes RV, Giussani DA, *et al.* Cardiovascular function in term fetal sheep conceived, gestated and studied in the hypobaric hypoxia of the Andean altiplano. *J Physiol* 2016;594:1231–1245.
38. Orgeig S, McGillick EV, Botting KJ, Zhang S, McMillen IC, Morrison JL. Increased lung prolyl hydroxylase and decreased glucocorticoid receptor are related to decreased surfactant protein in the growth-restricted sheep fetus. *Am J Physiol Lung Cell Mol Physiol* 2015;309: L84–L97.
39. Gonzaléz-Candia A, Candia AA, Ebensperger G, Reyes RV, Llanos AJ, Herrera EA. The newborn sheep translational model for pulmonary arterial hypertension of the neonate at high altitude. *J Dev Orig Health Dis* 2020;11:452–463.
40. Mandell E, Kinsella JP, Abman SH. Persistent pulmonary hypertension of the newborn. *Pediatr Pulmonol* 2021;56:661–669.
41. Stenmark KR, Fagan KA, Frid MG. Hypoxia-induced pulmonary vascular remodeling: cellular and molecular mechanisms. *Circ Res* 2006;99: 675–691.
42. Herrera EA, Pulgar VM, Riquelme RA, Sanhueza EM, Reyes RV, Ebensperger G, *et al.* High-altitude chronic hypoxia during gestation and after birth modifies cardiovascular responses in newborn sheep. *Am J Physiol Regul Integr Comp Physiol* 2007;292:R2234–R2240.
43. Roofthooft MT, Bergman KA, Waterbolk TW, Ebels T, Bartelds B, Berger RM. Persistent pulmonary hypertension of the newborn with transposition of the great arteries. *Ann Thorac Surg* 2007;83: 1446–1450.
44. Thomas AR, Ma AL, Weinberg DD, Huber M, Ades A, Rychik J, *et al.* Delivery room oxygen physiology and respiratory interventions for newborns with cyanotic congenital heart disease. *J Perinatol* 2021;41: 2309–2316.
45. Maritz GS, Cock ML, Louey S, Suzuki K, Harding R. Fetal growth restriction has long-term effects on postnatal lung structure in sheep. *Pediatr Res* 2004;55:287–295.
46. Tan RC, Ikegami M, Jobe AH, Yao LY, Possmayer F, Ballard PL. Developmental and glucocorticoid regulation of surfactant protein mRNAs in preterm lambs. *Am J Physiol* 1999;277:L1142–L1148.
47. Braems GA, Yao L-J, Inchley K, Brickenden A, Han VK, Grolla A, *et al.* Ovine surfactant protein cDNAs: use in studies on fetal lung growth and maturation after prolonged hypoxemia. *Am J Physiol Lung Cell Mol Physiol* 2000;278:L754–L764.
48. McGillick EV, Orgeig S, Morrison JL. Structural and molecular regulation of lung maturation by intratracheal vascular endothelial growth factor administration in the normally grown and placentally restricted fetus. *J Physiol* 2016;594:1399–1420.
49. Hume PS, Gibbings SL, Jakubzick CV, Tuder RM, Curran-Everett D, Henson PM, *et al.* Localization of macrophages in the human lung via design-based stereology. *Am J Respir Crit Care Med* 2020;201: 1209–1217.
50. Hsia CC, Hyde DM, Ochs M, Weibel ER; ATS/ERS Joint Task Force on Quantitative Assessment of Lung Structure. An official research policy statement of the American Thoracic Society/European Respiratory Society: standards for quantitative assessment of lung structure. *Am J Respir Crit Care Med* 2010;181:394–418.